ADVANCED FUNCTIONAL MATERIALS
www.afm-journal.de

Amyloid Directed Synthesis of Titanium Dioxide Nanowires and Their Applications in Hybrid Photovoltaic Devices

*Sreenath Bolisetty, Jozef Adamcik, Jakob Heier, and Raffaele Mezzenga**

This paper reports β-lactoglobulin amyloid protein fibrils directed synthesis of Titanium Dioxide (TiO_2) hybrid nanowires. Protein fibrils act as templates to generate closely packed TiO_2 nanoparticles on the surface of the fibrils using titanium (IV) bis (ammonium lactato) dihydroxide (TiBALDH) as precursor, resulting in the TiO_2–coated amyloid hybrid nanowires. These amyloid fibrils also exhibit complexation with a luminescent water-soluble semiconductive polythiophene (P3HT). TiO_2 nanowires behave as electron acceptor while, P3HT as electron donor. In this way, amyloid-TiO_2 hybrid nanowires can serve in heterojunction photovoltaic devices. To demonstrate this, a photovoltaic active layer is prepared by spin coating the blended mixture of polythiophene-coated fibrils and amyloid-TiO_2 hybrid nanowires. The current–voltage characteristics of these photovoltaic devices exhibit excellent fill factor of 0.53, photovoltaic current density of 3.97 mA·cm^{-2} and power conversion efficiency of 0.72%, highlighting a possible future role for amyloid-based templates in donor–acceptor devices, organic electronics and hybrid solar cells.

1. Introduction

Biomolecules have unique possibility to direct the synthesis of inorganic materials via biomineralization processes.[1] Examples include the formation of silicates, calcium carbonate and apatite.[2] Proteins and peptides can facilitate "green" synthesis of these inorganic materials, and thus stand as an alternative to the conventional synthesis relying on harsher conditions (e.g. high temperature, pressure or pH).[3] Biomolecule-directed synthesis of TiO_2 (Titanium dioxide) has attracted special interest due to the numerous related applications such as photo catalysts, gas sensors, pigments, lithium batteries and solar cells.[4] For example, Silicatein filaments were utilized for the formation of TiO_2 using the Ti- precursor compound [titanium (IV) bis-(ammonium lactato-) dihydroxide (TiBALDH)].[5] Additionally, synthesis of the TiO_2 from precursor solutions exposed to peptide R5,[6] polyallylamine,[7] spermidine and spermine[8] has also been reported. In this work, we report on the formation of the TiO_2 hybrid nanowires using amyloid β-lactoglobulin protein fibrils, and we show how these hybrids materials can serve in optoelectronic applications.

Amyloids are highly ordered protein/peptide self-assembled fibrillar nanostructures.[9] The biocompatibility and unique properties of the amyloids fibrils make them suitable for many bio-nanotechnological applications.[10] For example, amyloid fibrils have been already reported to act as templates for synthesis of inorganic nanowires, scaffolds for 3D cell culture and tissue engineering,[11] as precursors for silver nanowires, gold single crystals,[12] gold-silver alloys and composite conductive nanowires.[13] To the best of our knowledge, however, synthesis of the TiO_2 nanowires using β-lactoglobulin protein fibrils as templates, and their application in heterojunction hybrid solar cells has not yet been reported.

In view of the high electron mobility associated with inorganic materials, and their physical and chemical stability, hybrid heterojuction solar cells combining n-type organic material with inorganic nanomaterials show great promise in future energy conversion devices.[14] Thus, given the inexpensive precursors used in the present work, hybrid heterojuction solar cells based on amyloid-directed TiO_2 nanowires can offer an appealing additional step in the emerging field of photovoltaics.[15–17]

2. Results and Discussions

β-lactoglobulin is a globular milk protein which forms the semiflexible long linear amyloid fibril structures by the heat treatment at high temperature and low pH conditions. Detailed characterization of β-lactoglobulin protein fibrils has been described in earlier reports of our group.[18,19] **Figure 1**a shows a typical atomic force microscopy (AFM) image of semiflexible β-lactoglobulin fibrils, which are polydisperse in length with an average contour length of the order of several μm and a diameter less than 8 nm. In-depth analysis by AFM confirmed the expected periodic pitch along their contour length arising from the multistranded twisting of the protofilaments.[19] In order to use these fibrils as templates for TiO_2 nanowires, 700 μl of 0.1 wt.% β-lactoglobulin fibril solutions are mixed with 50 μl of 1 wt.% TiBALDH aqueous solution. The solution is very stable

Dr. S. Bolisetty, Dr. J. Adamcik, Dr. J. Heier, Prof. R. Mezzenga
ETH Zurich
Food and Soft Materials Science
Institute of Food
Nutrition and Health
CH-8092 Zurich, Switzerland
E-mail: raffaele.mezzenga@hest.ethz.ch
Dr. J. Heier
EMPA, Laboratory for Functional Polymers
Swiss Federal Laboratories for Materials Testing and Research
CH-8600 Dübendorf, Switzerland

DOI: 10.1002/adfm.201103054

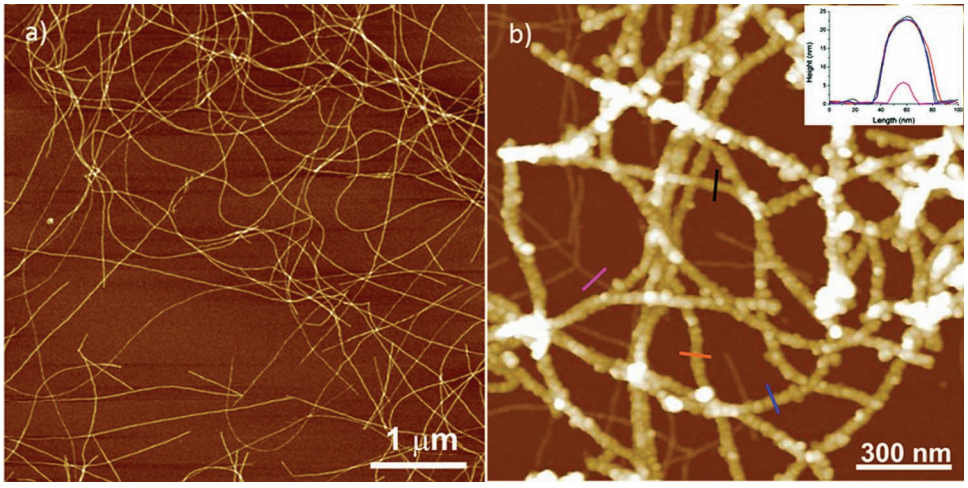

Figure 1. a) Atomic force microscope (AFM) image of the *β*-lactoglobulin amyloid fibrils showing long linear semiflexible structures with polydisperse contour lengths. b) AFM image of titanium dioxide (TiO_2) decorating the surface of the amyloid fibrils. The inset of the figure describes the height variation prior and after TiO_2 hybrid nanowire formation.

after mixing and sedimentation is not observed. Upon further addition of 50 μl, 1 wt.% TiBALDH, the protein fibrils solution starts to exhibit mild turbidity. The reaction mixture was kept at room temperature conditions for 1 hour with slow agitation to avoid random aggregates. The resulting solution mixture was then characterized by AFM, X-ray diffraction (XRD) and scanning electron microscopy (SEM) techniques. Figure 1b shows the AFM image of the solution of TiBALDH-processed protein fibrils solution. It can clearly be appreciated that the negatively charged TiBALDH precursor complexes with the positively charged protein fibrils, resulting in the synthesis of TiO_2 nanoparticles on the surfaces of the protein fibrils. Importantly, the titanium nanoparticles were sintering uniformly thus to yield a rather homogeneous layer of thickness of 20–25 nm decorating the surface of the protein fibrils. The inset of the Figure 1b reveals the change in the height of the uncoated and the coated protein fibrils at various locations. The average height of the protein fibrils is changed from the uncoated average 5 nm thickness to the TiO_2-coated fibril thickness of 23 nm. In order to understand the role of the *β*-lactoglobulin protein in the nanoparticles formation, we also prepared mixtures of pure *β*-lactoglobulin protein monomers solution at pH 2 with TiBALDH precursor solution. The AFM image (Figure S1 of the supporting information) exhibits uniform TiO_2 nanoparticles formation. The possible mechanism for the biomolecule-mediated TiO_2 nanoparticles synthesis is likely to follow closely that suggested by Kroger et al.[20] Initially, anionic TiBALDH molecules bind to the amino groups of the proteins and peptides through combination of electrostatic and hydrogen bond interactions. Then, the reaction follows the acid-base catalysis of the protein/peptide molecules leading to the hydrolysis of the TiBALDH complexes, followed by condensation of Ti-hydroxyl species, ultimately resulting in the synthesis of the TiO_2 nanoparticles. Dickerson and colleagues pointed out that the increase in the number of positive charges carried by the peptides increases the amount of the TiO_2 formation.[21] In our case, the *β*-lactoglobulin protein fibrils are highly positively charged at pH 2 and hence, optimize the formation of the TiO_2. Further, polymorphism of the formed TiO_2 was characterized using XRD. XRD data of the TiO_2 *β*-lactoglobulin protein fibrils are shown in Figure S2 (see supporting information). This analysis confirms the crystalline anatase TiO_2 form having characteristic diffraction peak at 2θ of 25.25°. The SEM images further confirm homogeneous coating of TiO_2 on the surface of the protein fibrils even at the lower TiBALDH concentration (Figure S3 of the supporting information). Finally, the measurements by energy dispersive X-ray spectroscopy (EDX) provide a definitive confirmation of the TiO_2 composition of the inorganic layer coating the amyloid fibrils (Figure S4 of the supporting information).

Complexation of semiconductive polymers to biological molecules and macromolecules has the possibility to enhance the optical and electrical properties of the biological templates. For example, it has already been shown that DNA can be combined with *π*-conjugated polymers[22] to enhance their conductive properties. Hamedi et al. self-assembled conjugated polymer onto the surface of insulin fibrils to yield electrically conductive active networks.[23] Here, we exploit again the positive linear charge density of the *β*-lactoglobulin protein fibrils, to electrostatically complex them with a counter charged water soluble modified polythiophene (sodium poly [2-(3-thienyl) ethoxy-4-butylsulfonate]; for the chemical structure see Figure S5 in the supporting information). Complexes obtained by mixing solutions of 0.1 wt.% protein fibrils with 0.5 wt.% polythiophene are stable over several weeks and sedimentation is not observed. The morphology of the resulting complexes was investigated by TEM. A necklace configuration of small globular particles of polythiophene decorating the *β*-lactoglobulin amyloid fibrils is found (**Figure 2**a). This is in perfect agreement with the morphological characterization of other types of electrostatic complexes of *β*-lactoglobulin amyloid fibrils and sulfated polysaccharides.[24] Similarly, increasing the ratio of conductive polymer to the fibrils results in larger amount of the globular particles on the surface of the protein fibrils. Because polythiophenes are known to exhibit excellent luminescence properties, we checked first by confocal laser-scanning microscopy whether,

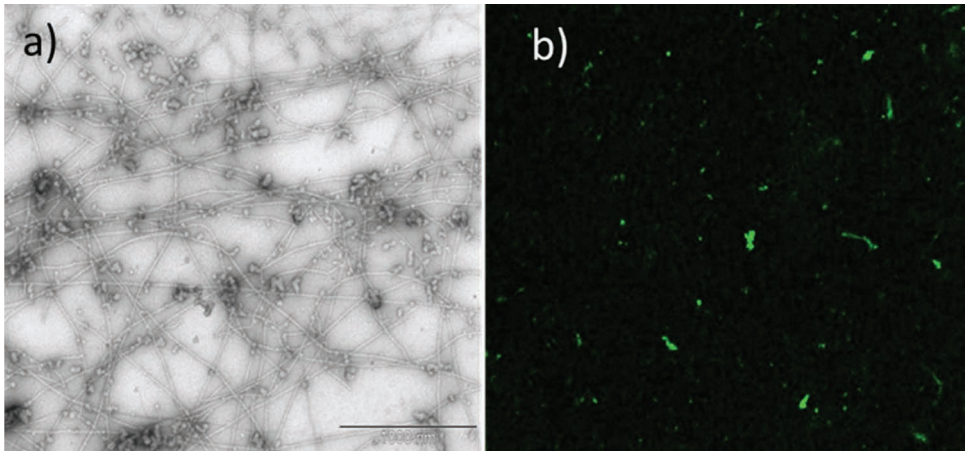

Figure 2. a) Transmission electron microscope (TEM) image of the β-lactoglobulin amyloid fibrils incubated with the sulfated polythiophene, showing a necklace morphology of polythiophene globules decorating amyloid fibrils (scale bar is 1000 nm). b) Confocal laser-scanning microscopy image of the β-lactoglobulin amyloid fibrils incubated with the sulfated polythiophene.

after complexation, also the polythiophenes-protein fibril complexes emit light upon excitation. Excitation was performed at a wavelength of 363 nm, and the corresponding emission was collected at a wavelength of 576 nm (see supporting information Figure S6). Figure 2b clearly displays the light emission from the polythiophene-coated β-lactoglobulin fibrils.

Fluorescence emission measurements were performed with the blended mixture of the 1 wt.% polythiophene and different concentrations of TiO_2-amyloid hybrid nanowires (See supporting information Figure S7). Fluorescence quenching is clearly observed and quenching is dependent on the concentration of TiO_2-amyloid hybrid nanowires, indicating electron transfer between the polythiophene (donor) and the TiO_2-amyloid hybrid nanowires (acceptor). The results of this experiment suggest the possibility to generate solar power with these materials.

The solar cell device was then prepared by fabricating the active layer composed of the TiO_2-amyloid hybrid nanowires blended with the water-soluble polythiophene. In this scheme, TiO_2-hybrid nanowires acted as electron acceptor while water-soluble polythiophene acted as electron donors. **Figure 3** summarizes schematically the architecture of the photovoltaic device. The device was prepared by depositing the various layers by spin coating on the indium-tin-oxide (ITO) glass substrate, where the ITO layer was used as anode. Poly 3,4-ethylenedioxy thiophene-poly styrene sulfonate (PEDOT-PSS) was the first layer (70 nm) spin coated onto ITO and had the role to promote extraction of hole charges. After deposition of this layer, the device was heated to 120°C for 12 minutes to remove residual water. On the top of the PEDOT-PSS layer, the active layer (35 nm) was then deposited by spin coating. It was composed by a blended mixture of polythiophene and TiO_2-amyloid hybrid nanowires in the following weight ratios 1:1, 4:1, 1:4, 1:8 and 1:18. In order to avoid short circuiting between the electrodes through pinholes in the active layer, an additional electron extracting layer of fullerene C60 (35 nm) was deposited on top of the active layer. This layer was deposited using a high vacuum deposition chamber placed in a glove box. In order to secure good contact between the C60 layer and the aluminum cathode layer, a 2 nm thick AlQ_3 [tris(8-hydroxyquinoline) aluminium] layer was vapor deposited, after which, the aluminum cathode layer was finally deposited on top of the device by vacuum evaporation. A total of 8 solar cells with surface area of 0.031 cm^2 and 0.071 cm^2 on each glass substrate were produced to allow averaging of their optoelectronic performance. The hybrid solar cell characteristics were measured under both dark light as well as solar illumination at AM (air mass) 1.5, 100 $mW \cdot cm^{-2}$ using a Spectra Nova cell tester.

The device active layer was prepared by spin coating the solution of TiO_2 nanowires (700 µl of 0.8 wt.% fibrils mixed with 100 µl of 0.5 wt.% of TiBALDH precursor) blended with 100 µl of 1 wt.% of water-soluble polythiophene solution.

Initial attempts at generating performing solar cells were unsuccessful due to excessive roughness of the active layer, short circuiting the device. This originated from the long protein fibrils, having the contour length of several µm, which caused high surface roughness of the active layer, degrading the solar cell efficiency. To solve this issue, the long amyloid fibrils were cut down into shorter fibrils using high-pressure homogenizer at 600± 100 bar, as reported in previous work.[25] Homogenization was performed over five cycles resulting into

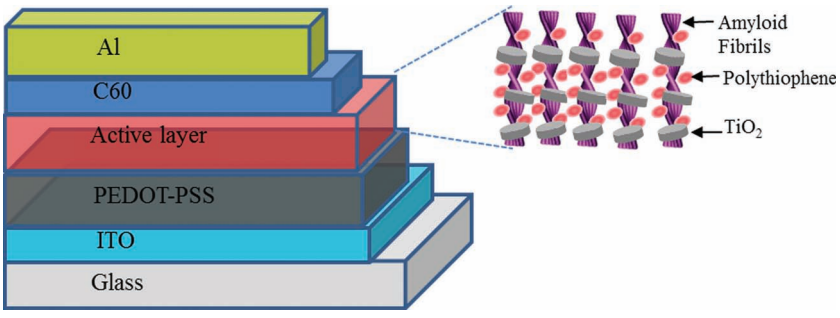

Figure 3. Schematic diagram of the hybrid photovoltaic device prepared using an active layer composed of the TiO_2-hybrid nanowires blended with polythiophene.

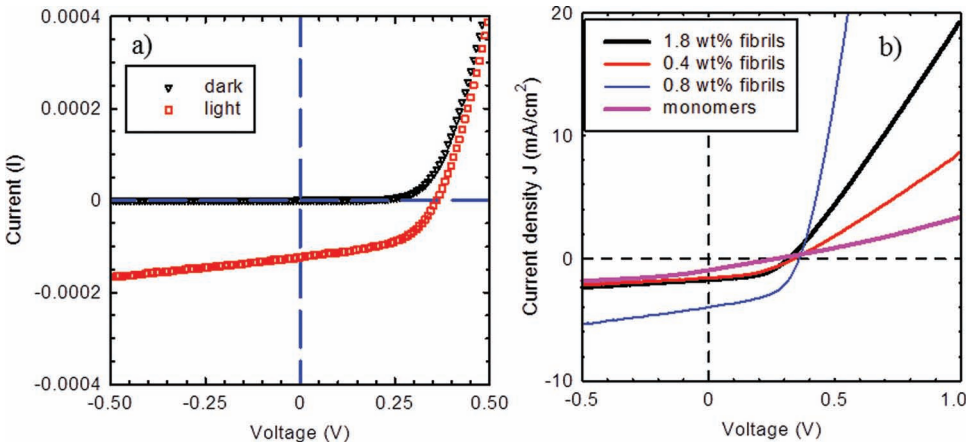

Figure 4. a) Current-voltage characteristics of the photovoltaic device having the active layer of 0.8 wt% TiO_2 protein fibrils blended with 1 wt% polythiophene. b) Current density and voltage characteristics of the solar cell active layers prepared with TiO_2-monomer hybrids or different concentrations of TiO_2-protein fibril hybrids.

an average contour length of 110 nm, and an identical cross section as the starting fibrils. These short protein fibrils were then used to direct the synthesis of the TiO_2–amyloid fibrils precursors and generate the active layer as discussed above. In Figure S8 of the supporting information, the AFM clearly demonstrates an efficient conversion of TiBALDH precursor into short TiO_2 nanowires using the high-pressure homogenized amyloid fibril templates, while Figure S9 (see supporting information) provides the UV-visible absorption spectra of the active layer based on the short nanowires-polythiophene complexes used for the preparation of the active layer of the device. The current-voltage characteristics of the photovoltaic device prepared using the active layer discussed above, are shown in **Figure 4**. The main photovoltaic device parameters achieved using this active layer are a short circuit current density (J_{sc}) of 3.97 mA·cm^{-2}, an open circuit voltage (V_{oc}) of 0.36 V, a fill factor of 0.53 and a power conversion efficiency (PCE) of 0.72%. Compared to the only two reports available to date, having considered amyloid fibrils in fully organic photovoltaic devices,[26,27] this represents more than a two-fold increase in efficiency. The best performance of the device is achieved at the protein fibril concentration of 0.8 wt.% and polythiophene of 1 wt.%. The current density and voltage characteristics of the solar cell active layer prepared with different protein fibril concentration are shown in Figure 4b. Decrease in the protein fibril concentration to 0.4 wt.% resulted in photovoltaic parameters of *Jsc* 1.59 mA·cm^{-2}, V_{oc} of 0.33 V, fill factor of 0.41 and a PCE 0.225%. This clearly highlights the crucial role of the protein fibrils in controlling the efficiency of the device performance. Further increase in protein fibrils concentration to 1.8 wt.% equally results in the decrease of PCE efficiency to 0.268%. In this case, the decrease in efficiency is due to the higher surface roughness of the active layer. Similarly, increasing the amount of the TiBALDH precursor for the preparation of the content of TiO_2 hybrid nanowires or increasing the amount of polythiophene for the active layer of solar cells does not improve the enhancement of the PCE of solar cells, as the optimal ratio between hole and electron transporters domains is then affected. Control reference experiments were performed using identical device setup and active layers made of TiO_2 nanoparticles generated from native proteins monomers, blended with identical quantities of the same polythiophenes. These reference devices performed with very low PCE of 0.06%, which clearly demonstrates the crucial role of the high aspect ratio of protein fibrils in charge transport across the active layer, and their potential in hybrid heterojunction solar cells. In addition, reference devices without a C60 layer were prepared, with the best performing active layer of 0.8 wt.% TiO_2-protein fibril hybrids blended with 1 wt.% polythiophene. The current density and voltage characteristics of the solar cell without C60 layer is shown in Figure S10 (see supporting information). The device still performed well without C60 layer and showed a diode characteristics, but the PCE was low (0.13%) in comparison to devices prepared with C60 layer. We want to stress that the reason for the low efficiency is majorly because of the poor film forming properties by the blended mixture of the polythiophene and the hybrid anatase TiO_2-protein nanowires. Most of the samples have pinholes and upon evaporation of the top-electrode without C60 layer shortcuts are created, countering the photocurrent. Even though some photovoltaic activity can also originate from the active layer-C60 interface, the C60 electron extraction layer is most indispensable to avoid shortcuts.

3. Conclusions

β-lactoglobulin amyloid protein fibrils can direct the mineralization of the TiO_2 nanowires from inorganic precursors by a bio-mineralization process. Furthermore, the high linear charge density of β-lactoglobulin protein fibrils can be exploited to electrostatically complex water-soluble counter charged semiconductive polythiophenes. Blending the electron acceptor TiO_2–amyloid fibril hybrid nanowires with the electron donor semiconductive polythiophenes allowed designing the active layer for hetero junction photovoltaic devices with a power conversion efficiency of 0.72%. This is the first example of a hybrid material based on an inorganic oxide, amyloid fibrils and π-conjugated polymers capable of serving in photovoltaic

solar cells with an efficiency comparable to that of fully organic homologue active layers.

4. Experimental Section

Materials: Bio-pure bovine β-lactoglobulin (lot JE 002-8-415) was kindly donated by Davisco Foods International (Le Seur, MN). β-lactoglobulin protein purification and the fibril formation were performed according to the procedure described by Jung and Mezzenga.[28] In brief, β-lactoglobulin protein solutions were purified by centrifugal filtration followed by dialysis for 5 days. After purification, the protein solutions were adjusted to pH 2 and lyophilized. The protein fibril formation was achieved by heat treatment of the 2 wt.% β-lactoglobulin solutions (pH 2) at 90 °C for 5 hours. Following the heat treatment, the solutions were quenched by immersing in ice water.

Titanium(IV) bis(ammonium lactato) dihydroxide (TiBALDH) precursor and conducting polymer poly(3,4-ethylenedioxythiophene) poly(styrenesulfonate) (PEDOT:PSS) were purchased from Sigma-Aldrich. Water soluble polythiophene (sodium poly[2-(3-thienyl)ethoxy-4-butylsulfonate]) (P3HT) was purchased from American Dye Source. The complete preparation of the hybrid solar cell is detailed in the discussion part.

Characterization Methods: Atomic force microscope (AFM) in tapping mode was carried out on a Multimode 8 Scanning Force Microscope (Bruker). MPP-11100-10 tips for tapping mode in soft tapping conditions were used (Bruker) at a vibrating frequency of 300 KHz. Images were simply flattened using the Nanoscope 8.1 software.

Transmission electron microscopy (TEM) was carried out by bright field TEM (FEI, model CM12, NL) operated at 100 kV. Powder X-ray diffraction (XRD) patterns were obtained using Cu-Kα radiation on a Panalytical XPert-PRO (Reflective Mode) equipped with a X'Celerator Scientific RTMS detector. UV–visible and fluorescence emission spectra were recorded on a Hitachi 3000 spectrophotometer. The photovoltaic current-voltage measurements were carried out on a Spectra-Nova cell tester unit under AM1.5 G conditions (Xenon arc lamp 1000 W, Air Mass 1.5 Filters from Oriel and power calibrated using a reference cell provided by ISE Freiburg). The typical area of each cell was 0.031 cm^2. Average film thicknesses of the layers on the glass substrate were measured by profilometry (ambios XP1). Field emission scanning electron microscope (FE-SEM) was carried out on Tecnai F30 FEG (FEI, Eindhoven, NL) operated at 300 kV, at a point-to-point resolution 0.19 nm and the imaging was achieved using high angle annular dark field detector (HAADF). Confocal laser-scanning microscopy (CLSM) was performed by CLSM Zeiss 510 Meta.

Supporting Information

Supporting Information is available from the Wiley Online Library or from the author.

Acknowledgements

The authors gratefully acknowledge Dr. William Kylberg and Dr. Gaetan Wicht (EMPA, Dübendorf) for assistance during the solar cell device fabrication and characterization. Also, the authors would like to thank Dr. Sujoy Kanti Ghosh (ETHZ), Stephan Handschin (EMEZ, Zurich) for assistance during XRD and TEM measurements.

Received: December 16, 2011
Revised: February 27, 2012
Published online: May 14, 2012

[1] H. A. Lowenstam, S. Weiner, *On Biomineralization*, Oxford University Press, Oxford **1989**.
[2] A. Sigel, H. Sigel, R. K. O. Sigel, *Metal Ions in Life Sciences, Biomineralization: From Nature to Application*, John Wiley And Sons, New York **2008**.
[3] M. B. Dickerson, K. H. Sandhage, R. R. Naik, *Chem. Rev.* **2008**, *108*, 4935.
[4] X. Chen, S. S. Mao, *Chem. Rev.* **2007**, *107*, 2891.
[5] J. L. Sumerel, W. J. Yang, D. Kisailus, J. C. Weaver, J. H. Choi, D. E. Morse, *Chem. Mater.* **2003**, *15*, 4804.
[6] S. L. Sewell, D. W. Wright, *Chem. Mater.* **2006**, *18*, 3108.
[7] K. E. Cole, A. N. Ortiz, M. A. Schoonen, A. M. Valentine, *Chem. Mater.* **2006**, *18*, 4592.
[8] K. E. Cole, A. M. Valentine, *Biomacromolecules* **2007**, *8*, 1641.
[9] I. Cherny, E. Gazit, *Angew. Chem. Int. Ed.* **2008**, *47*, 4062.
[10] T. P. J. Knowles, M. J. Buehler, *Nat. Nanotechnol.* **2011**, *6*, 469.
[11] S. Mankar, A. Anoop, S. Sen, S. K. Maji, *Nano Rev.* **2011**, *2*, 6032.
[12] S. Bolisetty, J. J. Vallooran, J. Adamcik, S. Handschin, F. Gramm, R. Mezzenga, *J. Colloid Interface Sci.* **2011**, *361*, 90.
[13] D. N. Woolfson, Z. N. Mahmoud, *Chem. Soc. Rev.* **2010**, *39*, 3464.
[14] W. U. Huynh, J. J. Dittmer, A. P. Alivisatos, *Science* **2002**, *295*, 2425.
[15] K. M. Coakley, M. D. McGehee, *Appl. Phys. Lett.* **2003**, *83*, 3380.
[16] Q. Qiao, J. T. McLeskey, *Appl. Phys. Lett.* **2005**, *86*, 153501.
[17] C. Y. Kuo, W. C. Tang, C. Gau, T. F. Guo, D. Z. Jeng, *Appl. Phys. Lett.* **2008**, *93*, 033307.
[18] J. Adamcik, J.-M. Jung, J. Flakowski, G. Dietler, R. Mezzenga, *Nat. Nanotechnol.* **2010**, *5*, 423.
[19] S. Bolisetty, J. Adamcik, R. Mezzenga, *Soft Matter* **2011**, *7*, 493.
[20] N. Kroger, M. B. Dickerson, G. Ahmad, Y. E. Cai, M. S. Haluska, *Angew. Chem. Int. Ed.* **2006**, *45*, 7239.
[21] M. B. Dickerson, S. E. Jones, Y. E. Cai, G. Ahmad, R. R. Naik, *Chem. Mater.* **2008**, *20*, 1578.
[22] L. Dong, T. Hollis, S. Fishwick, B. A. Connolly, N. G. Wright, *Chem. Eur. J.* **2007**, *13*, 822.
[23] M. Hamedi, A. Herland, R. H. Karlsson, O. Inganäs, *Nano Lett.* **2008**, *8*, 1736.
[24] O. G. Jones, S. Handschin, J. Adamcik, L. Harnau, S. Bolisetty, R. Mezzenga, *Biomacromolecules* **2011**, *12*, 3056.
[25] J.-M. Jung, R. Mezzenga, *Langmuir* **2010**, *26*, 504.
[26] S. Barrau, F. Zhang, A. Herland, W. Mammo, M. R. Andersson, O. Inganas, *Appl. Phys. Lett.* **2008**, *93*, 023307.
[27] J.-H. Lee, S. Kang, S.-G. Lee, J.-H. Jin, J. W. Park, S. M. Park, S. Jung, S. R. Paik, *Acta Biomater.* **2010**, *6*, 4689.
[28] J.-M. Jung, G. Savin, M. Pouzot, C. Schmitt, R. Mezzenga, *Biomacromolecules* **2008**, *9*, 2477.